

Ultrasound evidence for a two-component superconducting order parameter in Sr_2RuO_4

S. Benhabib^{1,†}, C. Lupien^{2,†}, I. Paul^{3,*}, L. Berges¹, M. Dion², M. Nardone^{1,A},
Zitouni¹, Z.Q. Mao^{4,5}, Y. Maeno^{4,6}, A. Georges^{7,8}, L. Taillefer^{2,6,*} and C. Proust^{1,6,*}

¹*Laboratoire National des Champs Magnétiques Intenses (CNRS),
EMFL, INSA, UGA, UPS), Toulouse 31400, France*

²*Institut Quantique, Département de physique & RQMP,
Université de Sherbrooke, Sherbrooke,
Québec, J1K 2R1, Canada*

³*Laboratoire Matériaux et Phénomènes Quantiques,
Université de Paris, CNRS, F-75013, Paris, France*

⁴*Department of Physics,
Kyoto University, Kyoto 606-8502, Japan*

⁵*Department of Physics,
The Pennsylvania State University,
University Park, PA 16803 USA*

⁶*CIFAR, Toronto, Ontario, M5G 1M1, Canada*

⁷*Center for Computational Quantum Physics,
Flatiron Institute, New York, NY 10010 USA*

⁸*Collège de France, 75005 Paris, France*

The quasi-2D metal Sr_2RuO_4 is one of the best characterized unconventional superconductors, yet the nature of its superconducting order parameter is still highly debated [1–3]. This information is crucial to determine the pairing mechanism of Cooper pairs. Here we use ultrasound velocity to probe the superconducting state of Sr_2RuO_4 . This thermodynamic probe is symmetry-sensitive and can help to identify the superconducting order symmetry [4, 5]. Indeed, we observe a sharp jump in the shear elastic constant c_{66} as the temperature is raised across the superconducting transition at T_c . This directly implies that the superconducting order parameter is of a two-component nature. Based on symmetry argument and given the other known properties of Sr_2RuO_4 [6–8], we discuss what states are compatible with this requirement and propose that the two-component order parameter, namely $\{d_{xz}; d_{yz}\}$, is the most likely candidate.

In conventional superconductors, the pairing mechanism originates in the interaction of electrons with phonons and the resulting superconducting order parameter has s -wave symmetry. The Fermi statistic imposes that the orbital symmetric state of two electrons must combine with an antisymmetric spin singlet part. Contrariwise, in superfluid ^3He , the ferromagnetic spin fluctuations being the mechanism responsible for pairing, the resulting spin states are triplet. In this case, the orbital part of two ^3He atoms has p -wave symmetry [9]. For 25 years, superconductivity of Sr_2RuO_4 has been viewed as an electronic analog of superfluid ^3He [1–3]. The initial report of the temperature independent spin susceptibility through T_c [10] and the indication of time-reversal symmetry breaking [11, 12] pointed to a spin triplet chiral p -wave order parameter. However, several experiments are in contradiction with this scenario [13], for example the lack of edge currents [14], the Pauli limiting critical field [15] and the absence of a cusp in the dependence of T_c on uniaxial strain [16]. Importantly, evidence of line nodes in the gap from specific heat [17], ultrasound attenuation [18] and thermal conductivity [6, 19] is not compatible with a chiral p -wave order parameter, that has no symmetry-imposed node (for a two-dimensional Fermi surface). Recently, measurements of the NMR Knight shift were carefully revisited

and a clear drop in the spin susceptibility below T_c was detected [7], pointing to an order parameter with even parity. As a result, the chiral p -wave order parameter is excluded and the nature of the superconducting state in Sr_2RuO_4 is now a wide open question.

Γ	Basis function	Strain component	Elastic constant
A_{1g}	$a(k_x^2+k_y^2)+bk_z^2$	$u_{xx}+u_{yy}, u_{zz}$	$(c_{11}+c_{12})/2, c_{33}$
A_{2g}	$k_x k_y (k_x^2 - k_y^2)$	none	none
B_{1g}	$k_x^2 - k_y^2$	$u_{xx} - u_{yy}$	$(c_{11} - c_{12})/2$
B_{2g}	$k_x k_y$	u_{xy}	c_{66}
E_g	$k_x k_z, k_y k_z$	u_{xz}, u_{yz}	c_{44}

TABLE I. Irreducible representation of the strain tensor for the D_{4h} point group.

Sound velocity is a powerful thermodynamic probe for order parameter. For propagation along high-symmetry directions of the crystal, the sound velocity is $v_s = \sqrt{\frac{c_{ij}}{\rho}}$ where ρ is the density of the material and c_{ij} are the elastic constants defined as the second derivative of the free energy F with respect to the strain u_{ij} . In the framework of Landau-Ginzburg theory of phase transition, the observation of a discontinuity in the elastic constant at the

superconducting transition is a consequence of the symmetry allowed coupling term between the order parameter Δ and the strain u , $\lambda|\Delta|^2u$, where λ is a coupling constant [20]. As part of the free energy, this coupling term is invariant under all the operations of the point group, i.e. it belongs to the A_{1g} representation. Table I lists the irreducible strains corresponding to the point group D_{4h} for the tetragonal symmetry of Sr_2RuO_4 (see the corresponding product table in the SI section 6). If the superconducting order parameter is one-component, then $|\Delta|^2$ belongs to the A_{1g} representation. Consequently, the strain variable u can only belong to the A_{1g} representation, i.e. it corresponds to a longitudinal sound wave. A jump in the longitudinal elastic constant is observed at T_c in many superconductors and is directly related to the jump in the specific heat at T_c and the strain dependence of T_c via the Ehrenfest relation [4]. If an unusual jump in the elastic constant associated with a shear mode (B_{1g} or B_{2g} representation) is detected at T_c , then it necessarily implies that the superconducting order parameter is multi-dimensional [4, 5, 21].

Based on these symmetry arguments, further developed in this paper, we have performed measurements of longitudinal and transverse sound velocities in Sr_2RuO_4 across the superconducting transition down to 40 mK. The initial measurements [22] have been confirmed only recently using a different spectrometer (see SI section 2) and by a complementary technique [23].

Elastic constant	\mathbf{k}	\mathbf{p}	Sound velocity (km/s)	Value (GPa)
c_{11}	[100]	[100]	6.28	233
c_{44}	[100]	[001]	3.41	68.2
c_{66}	[100]	[010]	3.3	64.3
$(c_{11}-c_{12})/2$	[110]	[1 $\bar{1}$ 0]	2.94	51

TABLE II. Definition of the different sound modes measured at $T = 4$ K. \mathbf{k} and \mathbf{p} stand for the propagation and polarization direction, respectively. Sound velocities were obtained at low temperature using the echo spacing.

Table II shows the different acoustic modes with the directions of sound propagation and polarization of the transducer. The value of the sound velocity is obtained from the echo spacing at low temperature ($T = 4$ K) and can be converted to elastic constants using $\rho = 5.95$ g/cm³. They are in good agreement with resonant ultrasound spectroscopy measurements [23–25]. Fig. 1a and Fig. 1b show the temperature dependence of the sound velocity for the longitudinal mode c_{11} and the transverse mode $(c_{11}-c_{12})/2$, respectively. Red circles (open squares) correspond to measurements in the superconducting (normal) state. Fig. 1c and Fig. 1d show the difference between the superconducting state and the normal state for the two modes. A discontinuity is expected at T_c for the longitudinal mode, c_{11} . We estimate the magnitude of this drop to be $\Delta c_{11}/c_{11} \approx 2$ ppm. This rough estimation is based on the Ehrenfest relation, that links the jump of the sound velocity with the jump of the spe-

cific heat and the strain dependence of T_c (see SI section 3). This small discontinuity at T_c is thus hidden by the strong softening of the longitudinal constant in the superconducting state (≈ 80 ppm between T_c and $T \rightarrow 0$). A similar, but even stronger softening is observed for the transverse mode $(c_{11}-c_{12})/2$, below T_c (Fig. 1b). These results are qualitatively in agreement with previous measurements [26, 27] but the absolute value of their elastic constants differs from ours [28].

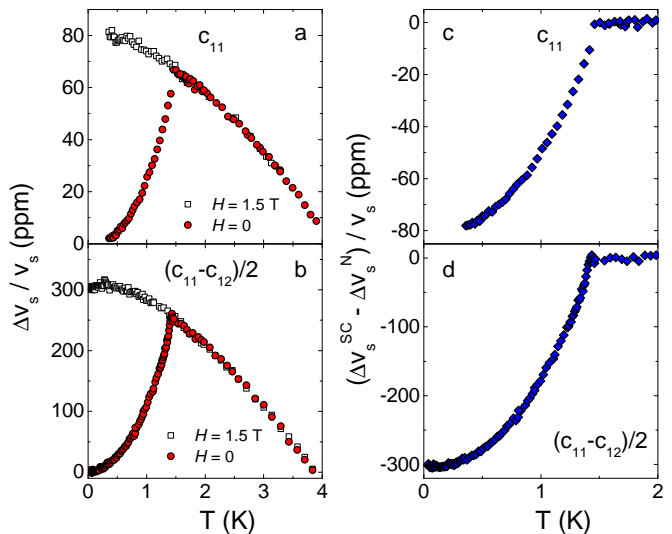


FIG. 1. **Relative change in the sound velocity of Sr_2RuO_4 through T_c .** Temperature dependence of the sound velocity for a) the longitudinal mode c_{11} measured at $f = 83$ MHz, b) the transverse mode $(c_{11}-c_{12})/2$ measured at $f = 21.5$ MHz. The normal state data (open squares) are obtained by applying a magnetic field of 1.5 T in the plane, larger than H_{c2} . The superconducting state data (red circles) are measured without any applied field. c) Difference between the superconducting state and the normal state, for the c_{11} mode. d) Same, for the $(c_{11}-c_{12})/2$ mode.

Fig. 2a shows the temperature dependence of the sound velocity for the transverse mode, c_{66} . The measurements in the superconducting state ($H = 0$, red circles) display a sharp discontinuity at the superconducting transition. The difference in the shear sound velocity between the normal and superconducting states (Fig. 2b) shows a small but very clear jump at T_c , of magnitude ≈ 0.2 ppm, 10 times larger than our experimental resolution. The exceptional sensitivity of our experiment is due to the very small attenuation of the c_{66} mode [18], which enabled us to detect up to ~ 60 echoes (see Fig. S1 in the SI) and to perform a fit on all of them.

Note that if there is any mixing of acoustic modes in the measurement, the small jump in c_{66} can easily be swamped by the huge softening of other modes. In a second experiment, using a different spectrometer, we were able to again detect the sharp drop below T_c in Sr_2RuO_4 , but with some contamination from other modes (see Fig. S2 in the SI). In the data of Fig. 2b, the complete lack of any temperature dependence below 1.3 K down to 0.04 K

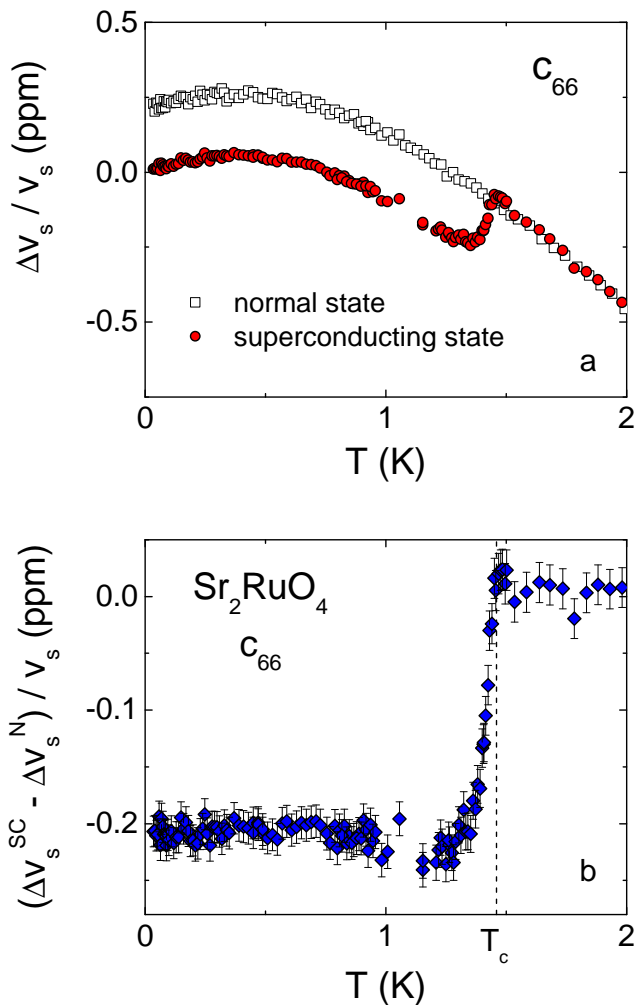


FIG. 2. **Jump in the c_{66} shear modulus at T_c .** a) Relative change in sound velocity for the transverse mode c_{66} measured at $f = 169$ MHz. The normal state data (open squares) are obtained by applying a field of 1.5 T in the plane. The superconducting state data (red circles) are measured without any applied field. b) Difference between the superconducting state and the normal state, for the c_{66} mode. A clear discontinuous jump is observed at T_c . The error bars are estimated from a constant voltage amplitude noise on the echoes measured by the phase comparator.

is strong evidence against such contamination.

This is the key finding of our study: we observe a sharp discontinuity at T_c in the sound velocity for the transverse mode c_{66} . This immediately provides unambiguous evidence that the superconducting order parameter must be of a two-component nature, consistent only with the E_g singlet representation, the E_u triplet representation or an accidentally degenerate combination of two one-dimensional representations.

A discontinuity of the sound velocity in the c_{66} mode at T_c of magnitude ≈ 10 ppm was recently detected in Sr_2RuO_4 also by resonant ultrasound spectroscopy performed at $f \sim 2$ MHz [23]. The difference in the mag-

nitude of the jump may come from a finite frequency effect on the dynamic of the order parameter. The consequence is a decrease of the amplitude of the anomaly as the frequency increases (see SI section 4 and Ref. [4]). Note that a rough estimation of the magnitude of the c_{66} drop using the Ehrenfest relation is about 2 ppm (see SI section 3).

Let's now turn on the Landau theory describing the strain-order parameter coupling. Sr_2RuO_4 has D_{4h} symmetry, and only the irreducible representation E of the point group is multi-dimensional. In this representation the superconducting order parameter is a two-component complex variable (Δ_A, Δ_B) . If the order parameter has E_u symmetry, (Δ_A, Δ_B) transform as (x, y) , and if the order parameter has E_g symmetry, they transform as (xz, yz) . For both cases, the Landau-Ginzburg free energy describing Δ and the uniform strains u is given by

$$F = F_\Delta + F_u + F_{\Delta-u}. \quad (1)$$

The superconducting part, expanded to fourth order, is

$$F_\Delta = a (|\Delta_A|^2 + |\Delta_B|^2) + \beta_1^0 (|\Delta_A|^2 + |\Delta_B|^2)^2 + \frac{\beta_2^0}{2} [(\Delta_A^*)^2 \Delta_B^2 + \text{c.c.}] + \beta_3^0 |\Delta_A|^2 |\Delta_B|^2.$$

The relevant elastic energy of the uniform strains is

$$F_u = \frac{1}{2} c_{11} (u_{xx}^2 + u_{yy}^2) + c_{12} u_{xx} u_{yy} + 2c_{66} u_{xy}^2 + \frac{1}{2} c_{33} u_{zz}^2 + c_{13} (u_{xx} + u_{yy}) u_{zz},$$

where c 's are the elastic constants in Voigt notation. The cross-coupling term is

$$F_{\Delta-u} = [\alpha_1 (u_{xx} + u_{yy}) + \alpha_2 u_{zz}] (|\Delta_A|^2 + |\Delta_B|^2) + \alpha_3 (u_{xx} - u_{yy}) (|\Delta_A|^2 - |\Delta_B|^2) + \alpha_4 u_{xy} (\Delta_A^* \Delta_B + \text{c.c.}).$$

The analysis of the above free energy is standard, and is described in detail in the SI (section 7). Similar expressions for the chiral p -wave state have been calculated by other groups [4, 5, 21]. Here we quote the main results.

For convenience we define $c_A \equiv (c_{11} + c_{12})/2$ and $c_O \equiv (c_{11} - c_{12})/2$. The latter is the orthorhombic elastic constant associated with the shear mode $u_{xx} - u_{yy}$, while c_{66} is the elastic constant of the monoclinic shear u_{xy} . Our aim is to calculate the jumps in the shear elastic constants defined by $\delta c \equiv c(T_c^-) - c(T_c^+)$.

The term $F_{\Delta-u}$ renormalizes the fourth order coefficients $\beta_i^0 \rightarrow \beta_i$ with

$$\begin{aligned} \beta_1 &= \beta_1^0 - \frac{1}{2} \left[\frac{\alpha_3^2}{c_O} + \frac{\alpha_1^2 c_{33} + \alpha_2^2 c_A - 2\alpha_1 \alpha_2 c_{13}}{c_A c_{33} - c_{13}^2} \right], \\ \beta_2 &= \beta_2^0 - \alpha_4^2 / (4c_{66}) \\ \beta_3 &= \beta_3^0 - \alpha_4^2 / (4c_{66}) + 2\alpha_3^3 / c_O. \end{aligned}$$

For the stability of the system, we need $\beta_1 > 0$, and $4\beta_1 \pm \beta_2 + \beta_3 > 0$. Within these ranges the following three superconducting phases are possible.

Case (1) Time reversal symmetry broken superconductor: In the region $\beta_2 > (0, \beta_3)$, we get the time reversal symmetry broken state with $(\Delta_A, \Delta_B) = \Delta_0(1, \pm i)$. In this phase, there is no spontaneous shear strain, and the tetragonal symmetry is preserved. The shear moduli jumps are

$$\delta c_{66} = \frac{-\alpha_4^2}{4\beta_2 + \alpha_4^2/c_{66}}, \quad (2a)$$

$$\delta c_O = \frac{-2\alpha_3^2}{\beta_2 - \beta_3 + 2\alpha_3^2/c_O}. \quad (2b)$$

Case (2) Nematic-monoclinic superconductor: In the region $\beta_2 < (0, -\beta_3)$, we get a nematic solution, $(\Delta_A, \Delta_B) = \Delta_0(1, \pm 1)$, which breaks the tetragonal symmetry by making the two in-plane diagonal directions inequivalent. It is accompanied by a spontaneous monoclinic strain, *i.e.* $u_{xy} \neq 0$. The shear moduli jumps are

$$\delta c_{66} = \frac{-\alpha_4^2/2}{4\beta_1 + \beta_2 + \beta_3 + \alpha_4^2/(2c_{66})}, \quad (3a)$$

$$\delta c_O = \frac{-2\alpha_3^2}{|\beta_2| - \beta_3 + 2\alpha_3^2/c_O}. \quad (3b)$$

Case (3) Nematic-orthorhombic superconductor: In the region $\beta_3 > (0, |\beta_2|)$, we also get a nematic solution, $(\Delta_A, \Delta_B) = \Delta_0(0, 1)$, or equivalently $\Delta_0(1, 0)$, which also breaks the tetragonal symmetry by making the two in-plane crystallographic axes inequivalent. It is accompanied by a spontaneous orthorhombic strain, *i.e.* $u_{xx} - u_{yy} \neq 0$. The shear moduli jumps are

$$\delta c_{66} = \frac{-\alpha_4^2/2}{\beta_2 + \beta_3 + \alpha_4^2/(2c_{66})}, \quad (4a)$$

$$\delta c_O = \frac{-\alpha_3^2}{2\beta_1 + \alpha_3^2/c_O}. \quad (4b)$$

Thus, in all three states the two shear elastic constants, c_{66} and c_O , jump at T_c . In our data, there is a clear jump in c_{66} . However, a jump in c_O could not be resolved, most likely because of the strong temperature dependence of $c_O(T)$ below the transition.

The observed jump in c_{66} at T_c implies that the superconducting order parameter of Sr_2RuO_4 is of a two-component nature. We now discuss the various implications of this new constraint, in the context of the other known properties of Sr_2RuO_4 .

(i) *Discrete symmetry breaking:* In a two-component scenario, the $U(1)$ symmetry breaking superconducting transition is necessarily accompanied by a simultaneous discrete symmetry breaking. For case (1), this discrete symmetry is time reversal leading to a spontaneous magnetization that can be detected in a μSR measurement,

for example. A non-zero μSR signal below T_c has indeed been reported [11], but its origin and implications are currently under investigation [29]. For cases (2) and (3), the broken symmetry is tetragonal D_4 leading to a monoclinic or an orthorhombic distortion of the tetragonal unit cell, respectively. In principle, it be detected through x-ray diffraction but no such distortion has been reported yet.

(ii) *Response to uniaxial pressure:* T_c as a function of the B_{1g} shear strain $u_{xx} - u_{yy}$ is expected to increase linearly. However experimentally, T_c increases quadratically with the uniaxial strain ϵ_{100} along [100], and therefore, the cusp at zero strain has not been observed. Note that, due to Poisson effect, ϵ_{100} is a combination of the B_{1g} shear $u_{xx} - u_{yy}$, and the in-plane A_{1g} longitudinal strain $u_{xx} + u_{yy}$. This implies that at quadratic order in ϵ_{100} , there is a B_{1g} perturbation that should lead to a splitting of the superconducting transition, if the order parameter is the $(1, i)$ or $(1, 1)$ type (see SI section 8). But for $(1, 0)$, one expects a single transition, with enhanced T_c . Since specific heat measurements detect no splitting of the superconducting transition under the application of strain (at least along the [100] direction) [8], the behavior of Sr_2RuO_4 under uniaxial pressure argues in favor of the $(1, 0)$ order parameter. (Here we assume that the strain-independent transition observed recently by zero-field muon spin relaxation [29] is not related to the superconducting state).

(iii) *Spin-wavevector content of Cooper pairs:* The drop of the Knight shift below T_c is strongly suggestive of an even parity order parameter [7, 30]. Assuming only intraband pairing, for singlets, the lowest harmonic is a d -wave solution $(\Delta_A, \Delta_B) = \Delta_0(k_x k_z, k_y k_z)$. For triplets, in order to be consistent with recent NMR as well as polarized neutron scattering data [31], the lowest harmonic triplet order parameter is the p -wave solution $(\Delta_A, \Delta_B) = \Delta_0 k_z (\hat{d}_x, \hat{d}_y)$.

(iv) *Line nodes:* Experimentally, thermal conductivity measurements show that the gap has vertical line nodes [6]. Whether the gap can also have horizontal line nodes is a quantitative question (see SI section 5). Recent data from quasiparticle interference (QPI) experiments are interpreted in terms of vertical line nodes along the diagonal[32], as in a $d_{x^2-y^2}$ state. Data on the variation of specific heat as a function of the angle of an in-plane magnetic field relative to the crystal have been interpreted either in terms of vertical line nodes of the $k_x k_z$ -type [33] (*i.e.* rotated by 45 deg compared to the $d_{x^2-y^2}$ state) or horizontal line nodes [34]. All states that we discuss within the E_g and E_u representations necessarily have horizontal line nodes. In the singlet sector (E_g), the states $(1, 0)$ and $(1, 1)$, which break tetragonal symmetry, also have vertical line nodes (respectively in the [100] and [110] directions). However, the state $(1, i)$, which breaks time reversal symmetry, typically does not have vertical line nodes, unless the pairing leads to a Bogoliubov Fermi surface [35]. In the triplet sector (E_u), the p -wave solutions do not have vertical line nodes. In

order to have triplet solutions also consistent with vertical line nodes one needs to consider a higher harmonic f -wave solution $(\Delta_A, \Delta_B) = \Delta_0 k_z (k_x^2 - k_y^2) (\hat{d}_x, \hat{d}_y)$.

(v) *Accidental degeneracy*: Until now, we only considered the two-dimensional irreducible representation E . In principle, one can also get a two-dimensional Δ if two one-dimensional representations become accidentally degenerate. The advantage of such a scenario is that it allows the possibility of having a finite jump in c_{66} while having no jump of c_O . Thus the $(s + d)$ -wave solution $(\Delta_A, \Delta_B) = (1, k_x k_y)$ will have the same free energy structure as in Eq. (1), except with $\alpha_3 = 0$. However, such a state is not guaranteed to have line nodes. Vertical line nodes are present for accidental degeneracy of higher order harmonics such as the $(d + g)$ -wave solution $(\Delta_A, \Delta_B) = (k_x^2 - k_y^2) (1, k_x k_y)$ [36].

If we put together the following arguments: 1) The superconducting order parameter has two components; 2) the gap has vertical line nodes (from thermal conductivity [6]); 3) the order parameter has even parity (from NMR [7]); 4) uniaxial strain does not split the superconducting transition (from specific heat under strain [8]). And if we disregard the evidence of time reversal symmetry breaking [11, 12, 29] then the only possible candidate is the $(1,0)$ state in E_g representation, namely the nematic state $k_x k_z$ (or $k_y k_z$), with both horizontal and vertical line nodes. The onset of this nematic state will be accompanied by an orthorhombic distortion of the lattice, and the formation of nematic domains. These structural changes should be detectable by x-ray diffraction measurements.

-
- [1] Maeno, Y. *et al.* Superconductivity in a layered perovskite without copper. *Nature* **372**, 532–534 (1994).
- [2] Rice, T. & Sigrist, M. J. Sr_2RuO_4 - an electronic analog of He-3. *Phys. Condens. Matter* **7**, L643-L648 (1995).
- [3] Mackenzie, A.P. & Maeno, Y. The superconductivity of Sr_2RuO_4 and the physics of spin-triplet pairing. *Rev. Mod. Phys.* **75**, 657-712 (2003).
- [4] Sigrist, M. Ehrenfest Relations for Ultrasound Absorption in Sr_2RuO_4 . *Progress of Theoretical Physics* **107**, 917-925 (2002).
- [5] Walker, M. B. & Contreras, P. Theory of elastic properties of Sr_2RuO_4 at the superconducting transition temperature. *Phys. Rev. B* **66**, 214508 (2002).
- [6] Hassinger, E. *et al.* Vertical line nodes in the superconducting gap structure of Sr_2RuO_4 . *Phys. Rev. X* **7**, 011032 (2017).
- [7] Pustogow, A. *et al.* Constraints on the superconducting order parameter in Sr_2RuO_4 from oxygen-17 nuclear magnetic resonance. *Nature* **574**, 72-75 (2019).
- [8] Li, Y.S. *et al.* High precision heat capacity measurements on Sr_2RuO_4 under uniaxial pressure. arXiv: 1906.07597 (2019).
- [9] Leggett, A.J. A theoretical description of the new phases of liquid ^3He . *Rev. Mod. Physics* **47**, 331 (1975).
- [10] Ishida, K. *et al.* Spin-triplet Superconductivity in Sr_2RuO_4 identified by ^{17}O Knight shift. *Nature* **396**, 658-660 (1998).
- [11] Luke, G.M. *et al.* Time-reversal symmetry-breaking superconductivity in Sr_2RuO_4 . *Nature* **394**, 558 (1998).
- [12] Xia, J. *et al.* A. High resolution polar Kerr effect measurements of Sr_2RuO_4 : Evidence for broken time-reversal symmetry in the superconducting state. *Phys. Rev. Lett.* **97**, 167002 (2006).
- [13] Mackenzie, A.P. *et al.* Even odder after twenty-three years: the superconducting order parameter puzzle of Sr_2RuO_4 . *npj Quantum Mat.* **2**, 40 (2017).
- [14] Kirtley, J.R. *et al.* Upper limit on spontaneous supercurrents in Sr_2RuO_4 . *Phys. Rev. B* **76**, 014526 (2007).
- [15] Deguchi, K. *et al.* Superconducting double transition and the upper critical field limit of Sr_2RuO_4 in parallel magnetic fields. *J. Phys. Soc. Jpn.* **71**, 2839-2842 (2002).
- [16] Hicks, C. W. *et al.* Strong increase of T_c of Sr_2RuO_4 under both tensile and compressive strain. *Science* **344**, 283-285 (2014).
- [17] Nishizaki, S., Maeno, Y., & Mao Z.Q. Changes in the superconducting state of Sr_2RuO_4 under magnetic fields probed by specific heat. *J. Phys. Soc. Jpn.* **69**, 572–578 (2000).
- [18] Lupien, C. *et al.* Ultrasound Attenuation in Sr_2RuO_4 : An Angle-Resolved Study of the Superconducting Gap Function. *Phys. Rev. Lett.* **86**, 5986-5989 (2001).
- [19] Suzuki, M. *et al.* Universal Heat Transport in Sr_2RuO_4 . *Phys. Rev. Lett.* **88**, 227004 (2002).
- [20] Rehwald, W. The study of structural phase transitions by means of ultrasonic experiments. *Advances in Physics* **22**, 721-755 (1973).
- [21] Contreras P. *et al.* Symmetry field breaking effects in Sr_2RuO_4 . *Revista Mexicana de Fisica* **62**, 442–449 (2016).
- [22] C. Lupien. Ultrasound attenuation in the unconventional superconductor Sr_2RuO_4 . PhD thesis (2002).
- [23] Ghosh, S. *et al.* Thermodynamic Evidence for a Two-Component Superconducting Order Parameter in Sr_2RuO_4 . arXiv: 2002.06130 (2020).
- [24] Paglione, J.P. *et al.* Elastic tensor of Sr_2RuO_4 . *Phys. Rev. B* **65**, 220506 (2002).
- [25] Barber, M.E. *et al.* Role of correlations in determining the Van Hove strain in Sr_2RuO_4 . *Phys. Rev. B* **100**, 245139 (2019).
- [26] Matsui, H. *et al.* Ultrasonic studies of the spin-triplet order parameter and the collective mode in Sr_2RuO_4 . *Phys. Rev. B* **63**, 060505R (2001).
- [27] Okuda, N. *et al.* Unconventional Strain Dependence of Superconductivity in Spin-Triplet Superconductor Sr_2RuO_4 . *J. Phys. Soc. Jpn.* **71**, 1134-1139 (2002).
- [28] Note that T. Suzuki and I. Ishii remeasured and confirmed recently the values of the elastic constants that are similar to the ones presented in the present paper.
- [29] Grinenko, V. *et al.* Split superconducting and time-reversal symmetry-breaking transitions, and magnetic order in Sr_2RuO_4 under uniaxial stress. arXiv: 2001.08152 (2020).

- [30] Ishida, K., Manago, M. and Maeno, Y. Reduction of the ^{17}O Knight shift in the Superconducting State and the Heat-up Effect by NMR Pulses on Sr_2RuO_4 . *J. Phys. Soc. Jpn* **89**, 034712 (2020).
- [31] Petsch, A.N. *et al.* Reduction of the spin susceptibility in the superconducting state of Sr_2RuO_4 observed by polarized neutron scattering. arXiv: 2002.02856 (2020).
- [32] Sharma, R. *et al.* Momentum Resolved Superconducting Energy Gaps of Sr_2RuO_4 from Quasiparticle Interference Imaging. *PNAS* **10**, 5222-5227 (2020).
- [33] Deguchi, K. *et al.* Gap Structure of the Spin-Triplet Superconductor Sr_2RuO_4 Determined from the Field-Orientation Dependence of the Specific Heat. *Phys. Rev. Lett.* **92**, 047002 (2004).
- [34] Kittaka, S. *et al.* Searching for Gap Zeros in Sr_2RuO_4 via Field-Angle-Dependent Specific-Heat Measurement. *J. Phys. Soc. Jpn* **87**, 093703 (2018).
- [35] Suh, H.G. *et al.* Stabilizing Even-Parity Chiral Superconductivity in Sr_2RuO_4 . arXiv: 1912.09525 (2019).
- [36] Kivelson, S.A. *et al.* A proposal for reconciling diverse experiments on the superconducting state in Sr_2RuO_4 . *npj Quantum Mat.* **5**, 43 (2020).
- [37] Mao Z.Q., Maeno Y. and Fukazawa H. Crystal growth of Sr_2RuO_4 . *Materials Research Bulletin*, **35**, 1813–1824, (2000).

METHODS

Samples

Our experiments were carried out on two oriented pieces cut from a single high-quality crystal of Sr_2RuO_4 grown by the travelling-solvent floating-zone technique[37]. T_c defined as the peak of the magnetic susceptibility is 1.4 K. Samples were polished to $1\ \mu\text{m}$ roughness, with two opposite faces whose parallelism was estimated to be better than $1.5\ \mu\text{m}/\text{mm}$. The alignment of the polished faces relative to the crystal axes was determined by Laue back reflection to be less than 0.5 deg off axis for the measurements shown in the main. One sample was aligned with the polished face perpendicular to (100) and the other sample was perpendicular to (110).

Ultrasound measurements

The measurements were performed with a pulse-echo technique using two home built spectrometers and commercial LiNbO_3 transducers. Most of the measurements were performed in a dilution refrigerator in Toronto [22] (by C. Lupien and C. Proust, in the Taillefer lab), with the transducer bonded to the crystals with a thin layer of optical coupling compound (Dow Corning 20-057).

The amplitude and the phase were measured using a phase comparator between a reference signal and the signal from the sample. The outputs of the phase comparator, I and Q , give the amplitude of the signal $A = \sqrt{I^2 + Q^2}$ and the phase $\phi = \arctan(Q/I)$.

The c_{66} mode was later re-investigated in a separate experiment, performed in Toulouse, using another spectrometer, in a ^3He refrigerator with the transducer bonded to the crystals with AngstromBond glue (AB9110). In this case, the amplitude of the signal was measured using a logarithmic amplifier. The phase was measured using a phase comparator but with a limiting amplifier at the input in order to have a perfect decoupling between the phase and the amplitude of the signal.

In the reflective configuration (using only one transducer), the sound wave propagates along the sample forward and is reflected back by the parallel opposite face, and hits again the same transducer. Fig. S1 shows an example of the amplitude of the signal for the c_{66} mode measured in Toronto. Each forward-and-back travel of the sound wave corresponds to one echo and up to 60 echoes were detected. The sound velocity variation is given by:

$$\frac{\Delta v_s}{v_s} = \frac{1}{\omega} \frac{\partial \phi}{\partial t} \quad (5)$$

where $\omega = 2\pi f$ and f is the frequency of the measurement. Since the phase is linearly increasing with time, we can perform a linear fit to the phase of different echoes versus time. By using all echoes in a weighted fit, the noise is reduced and the sensitivity of the measurement is close to 0.02 ppm.

Acknowledgements We thank J. Chang, C. Kallin, S. A. Kivelson, V. Madhavan, D. LeBoeuf, B. J. Ramshaw, G. Rikken, M. Sigrist, D. Vignolles and M. B. Walker, for helpful and stimulating discussions. Part of this work, associated with the PhD thesis of C.L. working with C.P. under the supervision of L.T., was performed at the University of Toronto. C.P. acknowledges support from the EUR grant NanoX n°ANR-17-EURE-0009 and from the ANR grant NEPTUN n°ANR-19-CE30-0019-01. L.T. acknowledges support from the Canadian Institute for Advanced Research (CIFAR) as a CIFAR Fellow and funding from the Natural Sciences and Engineering Research Council of Canada (NSERC; PIN: 123817), the Fonds de recherche du Québec - Nature et Technologies (FRQNT), the Canada Foundation for Innovation (CFI), and a Canada Research Chair. This research was undertaken thanks in part to funding from the Canada First Research Excellence Fund. Y.M. acknowledges support from JSPS Kakenhi (Grants JP15H5852, JP15K21717, and JP17H06136) and the JSPS-EPSRC Core-to-Core Program ‘‘Oxide-Superspin (OSS)’’.

Author Contributions C.L. and C.P. performed the ultrasound measurements in Toronto. S.B., L.B. and C.P. performed the ultrasound measurements in Toulouse. S.B., C.L., L.B., M.D. and C.P. analysed the data. I.P. performed the calculations, with the input of A.G. M.N. and A.Z. conceived and realized the ^3He cryostat in Toulouse. Z.Q.M and Y.M. prepared and characterized the Sr_2RuO_4 sample. I.P., L.T. and C.P. wrote the manuscript, in consultation with all authors. I.P., L.T. and C.P. co-supervised the project.

Competing interests The authors declare no competing interests.

Data availability All data that support the findings of this study are available from the corresponding authors on request.

† These authors contributed equally to this work.

* Correspondence and requests for materials should be addressed to I.P. (indranil.paul@univ-paris-diderot.fr), L.T. (louis.taillefer@usherbrooke.ca) or C.P. (cyril.proust@lncmi.cnrs.fr).